Practical Quadrupole Theory: Peak Shapes at Various Ion Energies

Randall E. Pedder
ABB Inc., Analytical-QMS Extrel Quadrupole Mass Spectrometry, 575 Epsilon Drive, Pittsburgh, PA 15238

(Poster presented at the 50th ASMS Conference on Mass Spectrometry and Allied Topics, Orlando, Florida, June 2 to 6, 2002)

At the 2001 ASMS conference, a graphical introduction to quadrupole theory was presented. (1) The solutions of the equations of motion for ions traversing through a quadrupole were illustrated, with simple X-Y plots used to illuminate the practical implications of the complex motion described by solving the Mathieu equation, specifically on resolution and mass calibration.

This presentation builds upon that graphical approach, using graphical depictions of calculated ion trajectories to illustrate the interaction of ion energy and frequency of ion motion, as well as the effect of a restricted exit aperture on experimentally measured peak shapes.

Practical examples of peak shape defects and their source are considered graphically, along with a simple theoretical explanation.

The goal of this work is to help build an intuitive understanding of how quadrupoles work, and more importantly, how to optimize performance in experiments involving quadrupoles.

Calculated ion trajectories are used to illustrate stability and instability (i.e. what happens if the ion going through the quadrupole is too light, too heavy or just right, based on the applied quadrupole voltages), as well as the consequences of too much ion energy (ions scream through the quadrupole even though they have theoretically unstable trajectories, resulting in poor abundance sensitivity, i.e. poor resolution at the baseline).

Peak shape defects due to excessive ion energy are well correlated to simulated ion trajectories. Quasi-stable trajectories of fast moving ions, which should be theoretically unstable, illustrate well the cause of poor abundance sensitivity in such cases.

I. INTRODUCTION

This presentation was created to address the following questions:

- What are some of the parameters that impact quadrupole mass peak shape?
- Why do quadrupole mass peaks tend to lift off the baseline on the low mass side of the peak more so than the high mass side of the peak?
- Why do mass peaks tend to have notches or splits when ion energy is increased, especially if the quadrupole is equipped with a restricted exit aperture?

An ion moving in an RF-only or RF/DC quadrupole field will exhibit periodic motion, with the frequencies and their relative magnitude easily calculated based on operating conditions.

The equations, which are used to describe this periodic motion, appear deceptively simple, but in practice, the correlation between the equations of motion and their calculated solutions is rich in its interpretation, if not obscure.

The purpose of this presentation is to de-mystify the theory associated with how quadrupoles operate, and to provide some practical application of theoretical quadrupole performance to experimentally measured peak shapes, specifically related to effects of ion energy on peak shapes, and the effect of a restricted exit aperture on peak shapes.

More thorough treatments of quadrupole theory can be found in Peter Dawson's book "Quadrupole Mass Spectrometry and its Applications". (2), and March and Hughes' book "Quadrupole Storage Mass Spectrometry". (3)

Analytical solutions to the Mathieu equation were calculated via successive approximation of continued fractions to yield a graph of the Mathieu stability diagram.

Runge-Kutta numerical integration of the Mathieu equation was used to generate simulated ion trajectories under various conditions.

Quadrupole mass peak shapes of Nitrogen (m/z 28) were measured with various ion energies and were correlated graphically to the analytical and numerical integration results, using a quadrupole constructed from 9.5 mm diameter rods operated at an RF frequency of 880 kHz, with a smaller than normal exit aperture (~3 mm diameter instead of the standard Extrel aperture of 7.5 mm).

This presentation approach is unique to any yet found in the literature, with its focus on practical implications of quadrupole theory, de-emphasizing the complex abstract equations typically utilized in traditional summaries of quadrupole theory.

II. THE EXPERIMENT

In a quadrupole mass spectrometer system, ions are somehow generated, focused into a quadrupole as close as possible to the centerline of the quadrupole axis, and are filtered while traveling through the quadrupole, with the resulting filtered ions traveling through an exit aperture to a detector or another analyzer. See Figure 1.

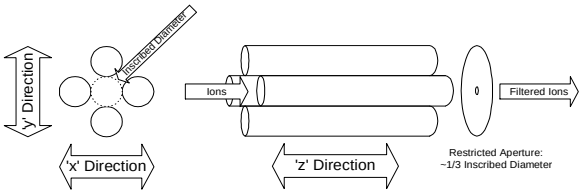

Figure 1. Schematic of quadrupole assembly identifying 'x', 'y', and 'z' directions, inscribed diameter, and ion flow.

Note that in this work, the exit aperture is restricted compared to the ideal in order to exaggerate the effects of ion energy noding.

Peak profiles are measured by scanning the RF and DC voltages along a scan line of appropriate ratio through the Mathieu stability diagram (i.e with approximately 6:1 RF to DC ratio).

Ion energy through the quadrupole ('z' direction) is calculated as the potential difference between the centerline offset potential of the quadrupole (pole bias) and the potential at which the ion was born (or had its last collision in the case of a high pressure source like a chemical ionization or electrospray source).

In this presentation, the 'x' and 'y' directions are identified as along the axes that connect the respective quadrupole pairs. Note that the assignment of one direction as 'x' and the other as 'y' is in practice somewhat arbitrary, and is really determined by the resolving DC polarity applied to the rod pairs.

Often, an aperture is placed at the exit of a quadrupole, either to shield a detector, or to serve as a conductance limit for a collision cell.

Ion trajectories were calculated via Runge-Kutta numerical integration of the Mathieu equation using a Turbo Basic program originally developed by the author at the University of Florida.

Iso-beta lines were calculated via successive approximation of the continued fraction solutions of the Mathieu equation. (4)

In this presentation, the system modeled and used experimentally had the following characteristics:

- Rod diameter: ~9.5 mm
- Inscribed diameter (distance between opposite rods): ~ 8.3 mm
- Aperture of Lens at exit of quadrupole: ~3 mm (Standard Extrel exit aperture for 9.5 mm quadrupole: 7.5 mm)
- Quadrupole length: ~20 cm
- RF frequency: 880 kHz
- Nitrogen ions at m/z 28

III. SOLVING THE EQUATIONS

The traditional treatment of quadrupole theory starts with a derivation of the Mathieu equation from 'F=ma' all the way through to the final parameterized form, with the following parametric substitutions:

$$\frac{d^2u}{d\xi^2} + (a_u - 2q_u \cos 2\xi)u = 0 \qquad a_u = \frac{8eU}{mr_0{}^2\Omega^2} \qquad q_u = \frac{4eV}{mr_0{}^2\Omega^2}$$

Extrel CMS L.P.
575 Epsilon Drive Pittsburgh, Pennsylvania 15238-2838 USA
Tel: (412) 963-7530 FAX: (412) 963-6578 Web: www.extrel.com

The *u* in the above equations represents position along the coordinate axes (x or y), ξ is a parameter representing Ωt/2, *t* is time, *e* is the charge on an electron, *U* is applied DC voltage, *V* is the applied zero-to-peak RF voltage, *m* is the mass of the ion, *r* is the effective radius between electrodes, and Ω is the applied RF frequency.

The rigorous analytical solution to this second order linear differential equation is:

$$u(\xi) = \Gamma \sum_{n=-\infty}^{\infty} C_{2n} \exp(2n+\beta)i\xi + \Gamma' \sum_{n=-\infty}^{\infty} c_{2n} \exp-(2n+\beta)i\xi$$

Which, intuitively obvious to any person skilled in the art, reduces to a similar infinite sum of sine and cosine functions:

$$u(\xi) = \sum_{n=-\infty}^{\infty} A_n \sin \omega_n + \sum_{n=-\infty}^{\infty} A_n \cos \omega_n$$

Where A_n is the amplitude and ω_n can be calculated as (n- β/2)*Ω.

In practice, the amplitudes for the center four frequencies of the infinite series (n=0, +1, -1, and +2) are large compared with the others, allowing us to truncate the solution as an approximation to:

$$u(\xi) = A_0 \cos \omega_0 + A_{+1} \cos \omega_{+1} + A_{-1} \cos \omega_{-1} + A_{+2} \cos \omega_{+2}$$

For example, consider the motion in the 'x' and 'y' directions for the position a=0.2306 and q=0.7001 in the first region of the Mathieu stability diagram. One could calculate β via successive approximation of the continued fraction solution as described by McLachlen (4) based on 'a' and 'q'. See Figure 2.

In this case, β_x = 0.918, yielding a trajectory in the 'x' direction that represents a beat pattern with large amplitudes at frequencies of 404 kHz and 476 kHz, with smaller amplitudes at frequencies of 1.284 MHz and 1.356 MHz.

Similarly, β_y = 0.0573, yielding a trajectory in the 'y' direction that features a large amplitude fundamental frequency of ion motion at 25 kHz, with slower amplitude harmonics at 855kHz and 905 kHz, with a tiny harmonic at 1.735 MHz (not shown in figure 2).

IV. MATHIEU STABILITY DIAGRAM

The traditional way to view the solutions of the Mathieu equation is to plot the calculated β values on one plot, connecting the points in a,q space that have the same β values (iso-β lines). See figures 3, 4 and 5

The most important of these iso-β lines are the ones that define the stability boundaries themselves, namely $\beta_x = 0$ and $\beta_x = 1$, and $\beta_y = 0$ and $\beta_y = 1$. It is interesting to note that the βx = 0 and βy = 0 boundaries which define the low mass side of the mass peak (left hand side of the stability diagram) are boundaries associated with low frequencies of ion motion (low frequency boundaries), while the $\beta_x = 1$ and $\beta_y = 1$ boundaries which define the high mass side of a mass peak (right hand side of the stability diagram) are high

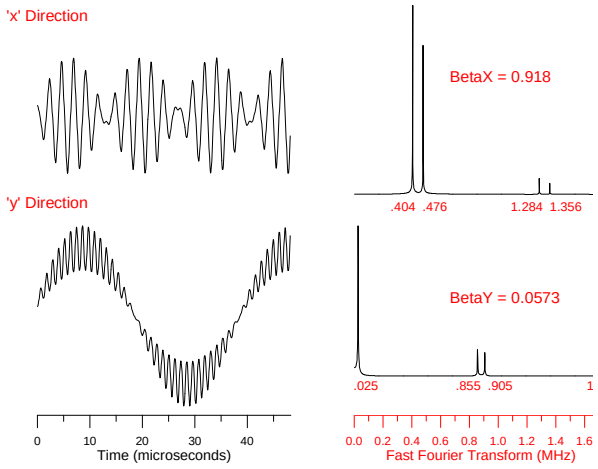

Figure 2. Ion trajectories with Fast Fourier Transform Spectra for a point on the stability diagram where a=0.2306 and q=0.7001 for m/z 28 with 2.5 eV ion energy. (Point C on Figure 5)

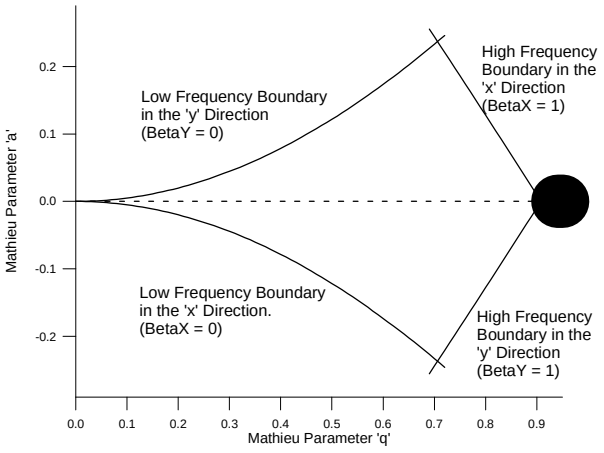

Figure 3. Mathieu Stability Diagram showing the first region of stability, which is two overlapping regions, one for the 'x' direction, and one for the 'y' direction.

Extrel CMS L.P.
575 Epsilon Drive Pittsburgh, Pennsylvania 15238-2838 USA
Tel: (412) 963-7530 FAX: (412) 963-6578 Web: www.extrel.com

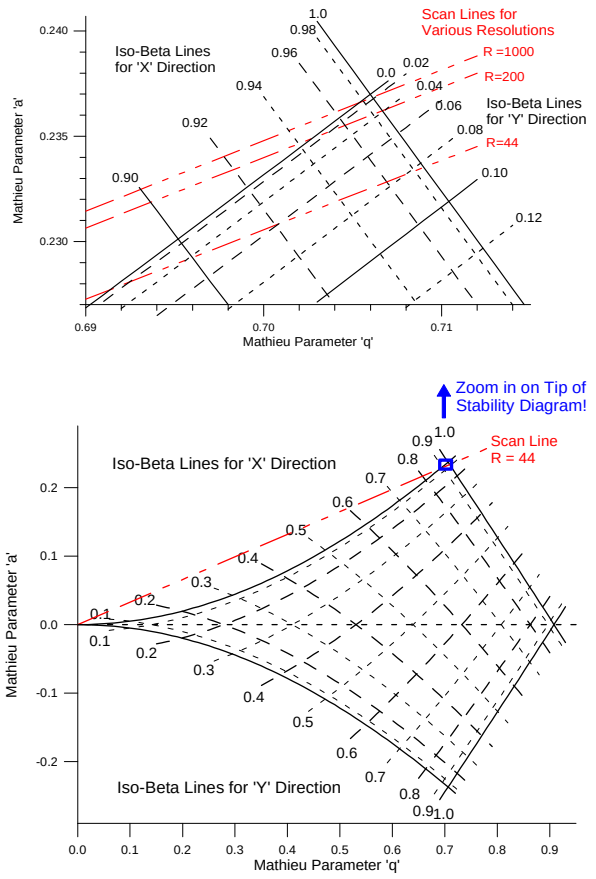

Figure 4. Mathieu Stability Diagram showing Iso-Beta lines, with zoom in view of tip, showing scan lines of various resolutions.

frequency boundaries.

By simply selecting an operating point in RF-DC space that is contained within this area bound by integer iso-beta lines (or one of the other regions of stability) will result in a theoretically stable trajectory, while operation outside these regions of stability will yield theoretically unstable trajectories.

Scanning the quadrupole voltages along a scan line through the stability diagram generates a mass peak. Figure 5 shows such a scan line, while figure 6 illustrates what the peak shape would look like for such a scan line.

V. SCANNING ACROSS MASS PEAK

When you scan through the stability diagram to generate a mass peak, you are sweeping the amplitude of the RF and DC voltages through the stability region for a given ion. This, in turn, changes the frequencies

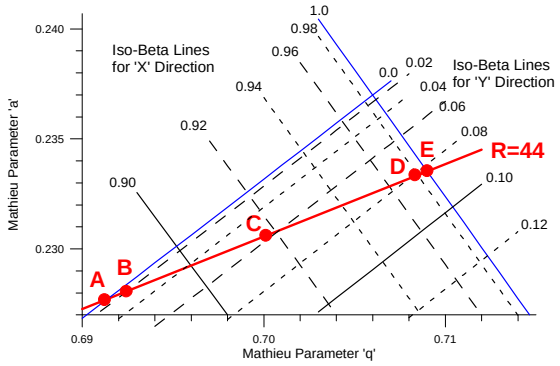

Figure 5. Scan line through the tip of the stability diagram that would yield slightly better than unit mass resolution (R=44) on mass 28.

of ion motion for ions of that mass through the quadrupole as can be calculated by solution of the Mathieu equation.

Figure 5 shows a stability diagram with a 'Resolution = 44' scan line, with five points identified as A, B, C, D, and E.

Point A corresponds to voltages in which the ion is stable in the 'x' direction, but unstable in the 'y' direction and gets ejected in the 'y' direction. This corresponds to the 'low frequency of ion motion boundary' on the low mass side of the peak. Note that the fundamental frequency trends to zero hertz and that the first and second harmonics converge toward the RF drive frequency as this boundary is approached!

Point E corresponds to voltages in which the ion is stable in the 'y' direction, but unstable in the 'x'

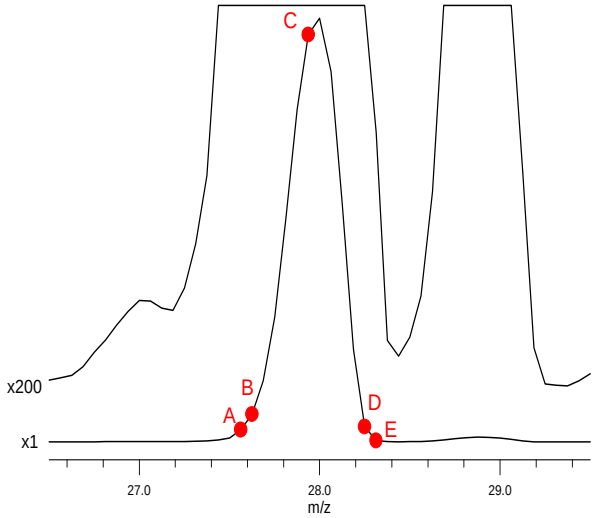

Figure 6. Experimental mass scan across mass 28 illustrating the relative intensities at the vabrious points along the scan line through the stability diagram shown in Figure 5.b

Extrel CMS L.P.
575 Epsilon Drive Pittsburgh, Pennsylvania 15238-2838 USA
Tel: (412) 963-7530 FAX: (412) 963-6578 Web: www.extrel.com

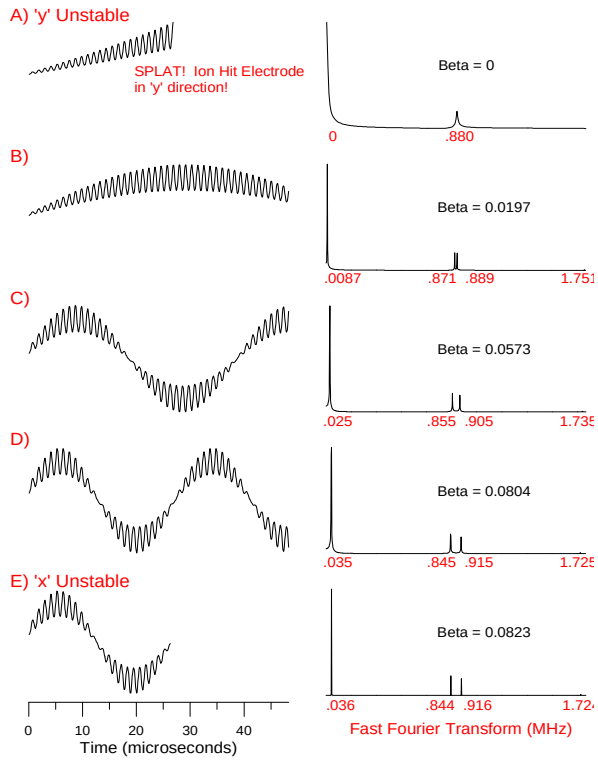

Figure 7. Trajectories of ions in the **'Y'** direction for various points along the scan line shown in Figure 5, with Fast Fourier Transforms showing frequencies of ion motion. Point A corresponds to the ion crossing the 'Low Frequency Boundary' in the 'Y' direction (low mass side of peak).

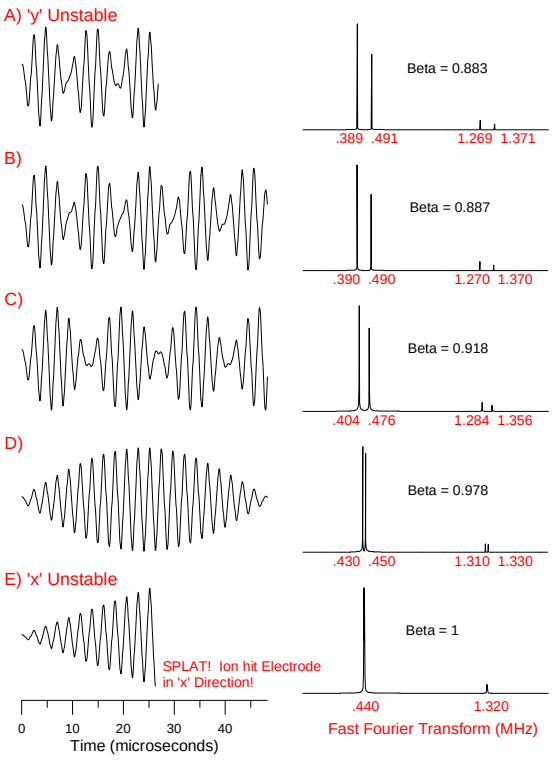

Figure 8. Trajectories of ions in the **'X'** direction for various points along the scan line shown in Figure 5, with Fast Fourier Transforms showing frequencies of ion motion. Point E corresponds to the ion crossing the 'High Frequency Boundary' in the 'X' direction (high mass side of peak).

direction and gets ejected in the 'x' direction. This corresponds to the 'high brequency of ion motion boundary' on the high mass side of the peak. Note that the Fundamental frequency of ion motion converges with the first harmonic at one half the RF drive frequency as this boundary is approached.

From Figure 5, it can be seen that the different points along the scan line correspond to different sets of βx and βy values. It follows that an ion would have different frequencies of ion motion at different points along the scan line, as shown in figures 7 and 8.

When ion energy is increased, the transit time through the quadrupole is decreased, effectively reducing the number of RF cycles (and hence the number of cycles of ion motion) that the ion sees as it transits through the quadrupole. Figure 9 shows this phenomenon, where the trajectory is 'stretched' or compressed, depending on whether the ion energy is increased or decreased.

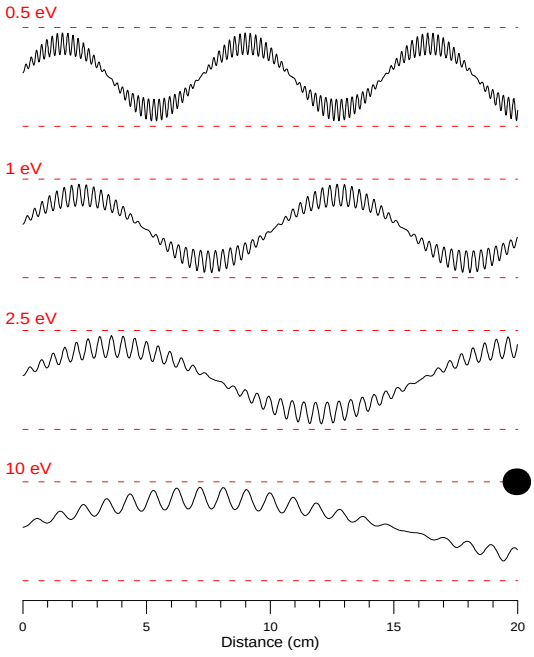

Figure 9. Calculated ion trajectories for an ion traveling through a quadrupole in the 'Y' direction at various ion energies (point C on figure 5.) The red dotted lines correspond to the quadrupole boundaries. The 'x' axis is distance along the quadrupole, not time.

Extrel CMS L.P.
575 Epsilon Drive Pittsburgh, Pennsylvania 15238-2838 USA
Tel: (412) 963-7530 FAX: (412) 963-6578 Web: www.extrel.com

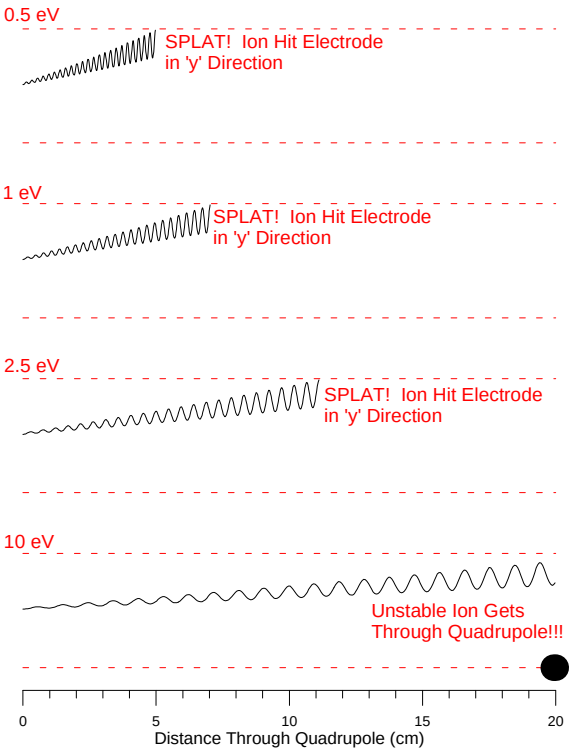

Figure 10. Calculated ion trajectories through the quadrupole in the 'y' direction for various ion energies, corresponding to point A from Figure 5, the low mass side boundary of the mass peak. Dotted red lines correspond to quadrupole boundaries.

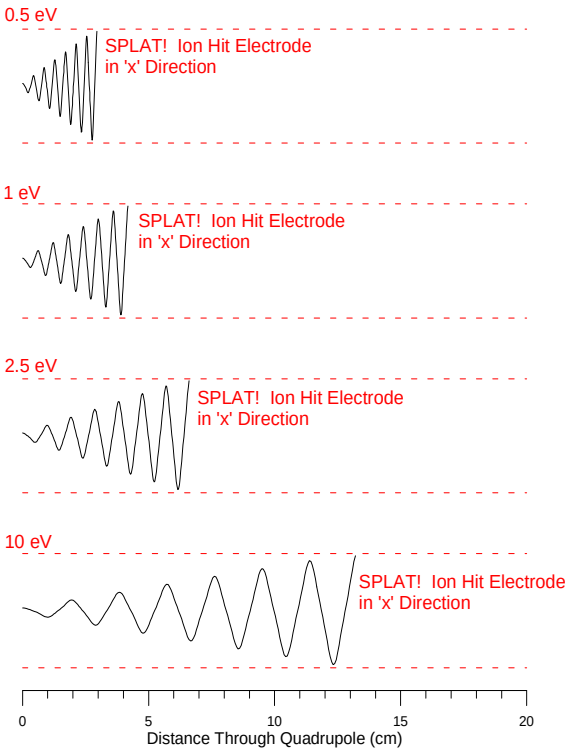

Figure 11. Calculated ion trajectories through the quadrupole in the 'x' direction for various ion energies, corresponding to point E from Figure 5, the high mass side boundary of the mass peak. Dotted red lines correspond to quadrupole boundaries.

VI. ION ENERGY EFFECTS ON ABUNDANCE SENSITIVITY

Abundance Sensitivity is a figure of merit that describes the ability of a mass spectrometer to discriminate between adjacent masses of widely different intensity. This is effectively a description of the resolution measured at the baseline. How much of the signal that is measured at mass 'M' is really attributable to 'M+1' or 'M-1'? How much do the masses leak into their neighbor's intensity measurement?

From figure 6, the m/z 28 peak looks well resolved in the 'x1' trace, but when magnified by 200, it can be seen that there is barely a separation between m/z 27 and m/z 28, while there is almost baseline separation between m/z 28 and m/z 29. This 'resolution at the baseline' is indeed a measure of the abundance sensitivity, which is typically identified as a fraction of the height of a given peak that appears one amu away from that mass peak. In this case the abundance sensitivity would be estimated at a few thousand.

Quadrupoles operated under normal conditions generally exhibit poorer abundance sensitivity on the low mass side of the peak than the high mass side of the peak (typically one order of magnitude difference). This difference in performance can be attributed to the fact that the low mass side of the peak corresponds to a 'fuzzy' low frequency boundary, while the high mass side of the peak corresponds to a sharper high frequency boundary.

Figures 10 and 11 illustrate the effects of varying ion energy at either of the low frequency boundary (Point A in Figure 5, illustrated in Figure 10), or the high frequency boundary (Point E in Figure 5, illustrated in Figure 11).

It is striking that on the low frequency boundary, ions can have 'quasi-stable' trajectories and get through the quadrupole, if the energy is sufficiently large, that they do not get a full cycle of ion motion, whereas we see more efficient rejection on the high mass side of the peak. This leads to the baseline liftoff that is more pronounced on the low mass side of a quadrupole mass peak.

VII. ION ENERGY PEAK SPLITTING

When a quadrupole has either an off-axis detector or a restricted exit aperture, it is possible to see nodes

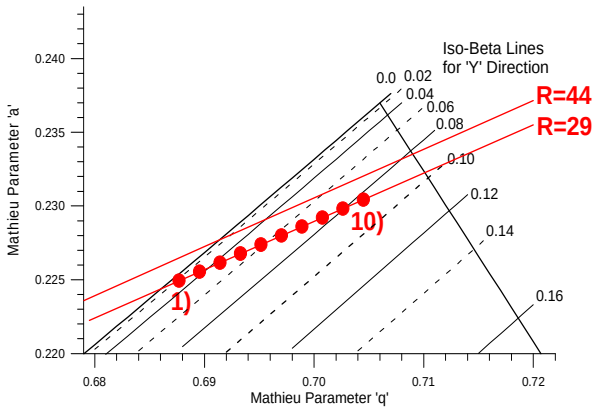

Figure 12. Stability diagram with only 'y' iso-beta lines identified. Points along R=29 scan line correspond with the peaks and valleys in Figure 13, as well as the trajectories in Figure 14.

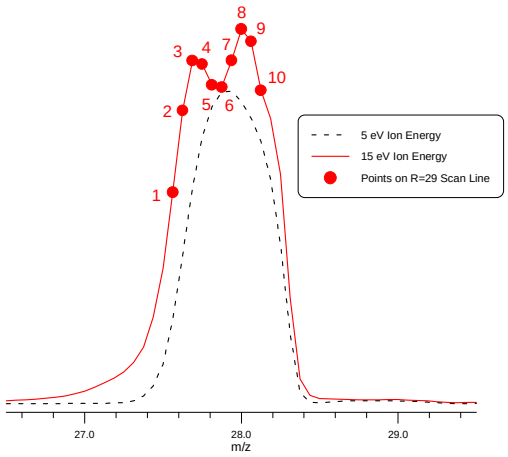

Figure 13. Unit mass resolution peak at two different ion energies.

appear in the quadrupole peak profile. Such peak splitting can be directly attributed to the periodic nature of ion motion through a quadrupole, and is generally sensitive to variation in ion energy. (i.e. if you change the ion energy, the relative location of the splits in the peak profile will change.)

A smaller than normal exit aperture (~3 mm instead of 7.5 mm) was inserted at the end of a quadrupole to exaggerate this effect for this presentation.

The quadrupole was tuned to nominally unit mass resolution (resolution = 29 for m/z 28), and ion energy was varied between 5 eV and 15 eV.

The scan line through the stability diagram is shown in Figure 12, with various points marked with large red dots. Only iso-β_y lines are shown, since peak splitting is attributed to low frequency 'y' motion.

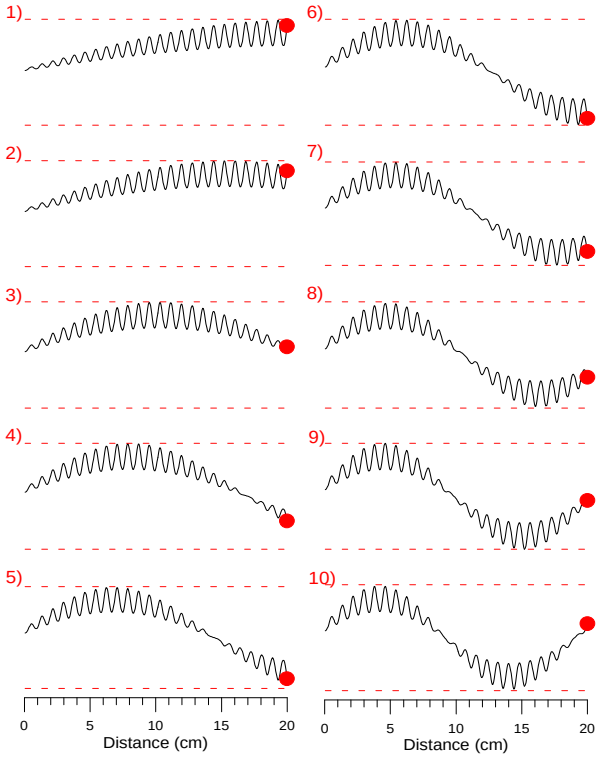

Figure 14. Ion trajectories in the 'y' direction for points along the scan line in Figure 12. Local maxima in the 15 eV spectrum shown in Figure 13 correspond to trajectories where the ion ended up in the middle of the quadrupole. The local minimum corresponds to trajectories in which the ion ends up far from the center of the quadrupole.

An experimentally collected mass peak profile is shown in Figure 13, with red dots marking the points correlating to the points on the scan line shown in Figure 12. Note that the β_y values change dramatically along the left hand side of the stability diagram, but more gradually as you move to the right hand side of the stability diagram. (the lines get further apart). This means that the frequency of ion motion changes much more dramatically on the low mass side of the peak, leading to more nodes on the low mass side of the peak, than on the high.

Figure 14 shows the trajectories that correspond to the ten red dots identified in Figures 12 and 13. Note the correlation between relative maxima and having the ions end up at the center of the exit of the quadrupole, and the correlation between the relative minimum of the mass peak corresponding to ions that end up nearer to the poles of the quad. The noding is a direct result of efficiency of transferring ions through the quadrupole exit lens. With a restrictive exit aperture, some of the stable ions do not reach the detector.

Extrel CMS L.P.
575 Epsilon Drive Pittsburgh, Pennsylvania 15238-2838 USA
Tel: (412) 963-7530 FAX: (412) 963-6578 Web: www.extrel.com

Abundance sensitivity is compromised with increased ion energy. Ions of the wrong mass can indeed travel through the quadrupole to the detector, with worse effects visible for 'too-heavy' ions contributing to the ion signal of the target mass on the low mass side of the mass peak. This effect is evidenced by the exhaggerated liftoff of the low mass side of the 15 eV ion energy peak profile in figure 13, as compared to the 5 eV peak profile in the same figure.

VIII. CONCLUSIONS

The purpose of this presentation is to help de-mystify the theory associated with how quadrupoles operate, specifically with regards to the effects of variation of ion energy on peak shape. Using this graphical approach, quadrupole operation can be understood intuitively without extensive study of the equations of motion.

Ion Motion in a quadrupole is periodic in nature, with abundance sensitivity on the low frequency ion motion / low mass side of the mass peak not quite as good as the abundance sensitivity on the high frequency ion motion / high mass side of the mass peak.

The ion motion at the stability boundary limits correspond to the convergence of the first and second harmonic to the RF drive frequency in the case of the low mass side of the peak / low frequency boundary, and the convergence of the fundamental and first harmonic to one half the drive frequency in the case of the high mass side of the peak / high frequency boundary.

Abundance sensitivity is the ultimate determinant of quadrupole resolution, with resolution at the baseline dictating the limit of resolution at half height. While resolution at half height remains virtually unchanged as ion energy is adjusted, the resolution at the baseline (abundance sensitivity) is very strongly dependent upon ion energy.

Resolving power is ultimately dictated by the number of cycles of ion motion that the ion sees as it traverses the quadrupole.

Increasing ion energy reduces the number of cycles of ion motion, and hence reduces resolution and abundance sensitivity.

Increasing rod length or RF frequency increases the number of cycles of ion motion and hence increases resolution and abundance sensitivity.

For the case of either restricted exit aperture or off-axis detector, too high an ion energy (or too narrow a range of ion energy) results in peak splitting or nodes in the mass peak, especially noticeable on the low-mass side of the mass peak.

IX. REFERENCES

1. Pedder R.E. *Practical Quadrupole Theory: Graphical Theory*, Extrel Application Note RA_2010, Poster presented at the 49th ASMS Conference on Mass Spectrometry and Allied Topics, Chicago, IL, 2001.
2. March, R.E., and Hughes, R.J. *Quadrupole Storage Mass Spectrometry*, Wiley Interscience, New York, 1989. Chapter 2: "Theory of Quadrupole Mass Spectrometry", Pages 31-110.
3. Dawson, P.H. *Quadrupole Mass Spectrometry and its Applications*, Elsevier, Amsterdam, 1976.
4. McLachlan, N.W. *Theory and Applications of Mathieu Functions*, Clarendon: Oxford, 1947.

Extrel CMS L.P.
575 Epsilon Drive Pittsburgh, Pennsylvania 15238-2838 USA
Tel: (412) 963-7530 FAX: (412) 963-6578 Web: www.extrel.com